1 December 1972, Volume 178, Number 4064

SCIENCE

Lunar Topography: Global Determination by Radar

Delay-Doppler stereoscopy and radar interferometry yield high-resolution three-dimensional views of the moon.

Irwin I. Shapiro, Stanley H. Zisk, Alan E. E. Rogers, Martin A. Slade, and Thomas W. Thompson

Introduction

Landing spacecraft on the lunar surface is a delicate affair; the moon's topography plays a vital role. Knowledge of this topography is important not only for lunar landing and exploration, but in order to solve a wide range of scientific problems on local to global scales. Precise information on absolute heights and local slopes is necessary for understanding mascons, rilles, fault lines, land slumping, and mare basins. These data are required to understand surface adjustments and their time scales, which can be interpreted in terms of the local subcrustal physical and mobility conditions. There are also important implications, for example, for lunar conditions at the time of formation of the basins; whether particular maria are highlands or lowlands depends on the time and gravitational circumstances under which they formed.

A comparison of surface-height variations where mascons are present with the variations in regions where they are absent may provide clues to differences in mechanical strength of different parts of the moon and may yield limits on the magnitude of regional radioactive heating and on the corresponding abundances of certain elements. Local slopes may clarify the origin of some rilles: Do they result from volcanic fissures or from aftereffects of impact phenomena?

The global—in contrast to the local—topography provides an essential boundary condition on the moon's overall physical structure, internal strength, composition, temperature, and energy budget. In many cases, the surface-height variations over the visible hemisphere provide a powerful tool for discriminating among theories of the moon's deep interior as well as of its origin and evolution. In combination with gravity-field data of comparable resolution, the topography makes it possible to infer departures of the moon's density distribution from hydrostatic equilibrium and to obtain answers to such questions as whether and to what extent conditions of isostasy prevail. Geodetic control on a global basis with an uncertainty of the order of 100 meters is desirable for many of these studies. Moreover, increased knowledge of the lunar topography will make it possible to pose sharper questions.

Current knowledge of lunar topography—both local and global—is based almost entirely on heliometer observations and the use of optical photogrammetry techniques. Despite decades of intensive effort, uncertainties of the order of 1 to 2 kilometers remain, the determinations being best near the center of the visible disk and worst near the limbs. The most serious deficiency is the lack of adequate control over the whole hemisphere (*1*). Our main purpose in this article is to describe new radar methods devised to obtain surface-height variations with higher accuracy and better global fidelity than has heretofore been possible (*2*). First we describe previous methods for mapping the moon with radar, and then the new techniques for adding altitude information to the radar map. Finally we present sample results for altitude contours on the moon obtained with the Haystack and Westford radar systems of the Massachusetts Institute of Technology (*3*).

Two-Dimensional Radar Photography: A Review

In contrast with an optical telescope, a single radar antenna has an angular resolution too crude to be useful for mapping. Hence, in radar observations of the moon reliance has been placed on the delay-Doppler principle (*4*). The round-trip echo time of a radar pulse provides one spatial coordinate of the reflecting region on the lunar surface. If the location and motion of the radar with respect to the center of mass of the earth are known, the reflecting region can be localized in a particular interval of distance from the origin of an earth-centered coordinate frame; this interval, in equivalent light time, is half the uncertainty in the measurement of the round-trip delay (*5*). The Doppler shift of the echo detected from the reflecting element on the lunar surface is proportional, in first order, to the projection of the element's apparent velocity (*6*), as viewed from the radar, in the direction of the radar site. Since the moon rotates as a rigid body, the

At the time this work was carried out, 1968 to 1970, Drs. Shapiro and Slade were associated with the Department of Earth and Planetary Sciences of the Massachusetts Institute of Technology, Cambridge 02139; Drs. Zisk and Rogers were with M.I.T.'s Haystack Observatory, Westford, Massachusetts 01886; and Dr. Thompson was with Arecibo Observatory, Puerto Rico. Drs. Slade and Thompson are now at Jet Propulsion Laboratory, Pasadena, California 91103.

Doppler-shift measurement (if we neglect parallax) serves to localize the reflecting region in a planar slab parallel to the plane containing both the vector from the radar to the moon's center of mass and the apparent angular velocity vector of the moon (*7*). The thickness of the slab is proportional to the uncertainty in the measurement of the radio frequency of the echo and inversely proportional to the total spread of Doppler shifts for the entire moon, the so-called limb-to-limb Doppler bandwidth.

To simplify further discussion, we will assume that contours of constant delay and contours of constant Doppler shift form two sets of planes, the first perpendicular to the radar-moon vector and the second parallel to it. The intersections are lines approximately perpendicular to the earth-moon direction, as shown in Fig. 1. Thus, the two-dimensional map is, in effect, a projection of the moon's surface onto a plane normal to the Doppler axis (*6*). This projection stands in contrast to ordinary photographs, which constitute projections onto the plane normal to the line-of-sight vector. Features on such two-dimensional radar maps represent, in analogy with ordinary photographs, simply the variation of reflectivity of the different elements on the surface. For radar maps, the illumination usually stems from the place at which the echo is detected; in optical photography, the source of illumination is usually the sun, and only at full moon does the photograph represent variations in backscattering as for radar.

To present radar maps so that they resemble optical photographs, it has been customary to assume that the moon is spherical and therefore to consider the intersection of a delay-Doppler "stick," or resolution cell, with the sphere as representing that part of the moon to which the echo power in the given delay-Doppler cell refers. Of course, each such cell, except for tangency conditions, intersects the sphere in two places. For the moon, the relatively small antenna beam can be used to resolve the ambiguity (see Fig. 1); for more distant planetary targets, other techniques can be employed (*8*). Because, at radar wavelengths, the moon and terrestrial planets behave partly as specular reflectors and partly as homogeneous diffuse reflectors, the average expected reflectivity for each cell is subtracted from the measured reflectivity. The resultant difference for each cell forms the basis for the radar map (*9*). A typical radar picture, shown in Fig. 2 (*10*), was obtained from radar signals at a wavelength of 3.8 centimeters; the circular polarization received was opposite to that transmitted. [For a specularly reflecting sphere, the reflected signal has a sense of circular polarization opposite to that of the incident wave; maps prepared from reflections with the same sense of polarization—the "depolarized" echoes—give information on the roughness of the target (*11*), since signals with this polarization must have been scattered by wavelength-sized material or undergone multiple reflections to have had the sense reversed again.]

Our discussion thus far has been limited to two-dimensional delay-Doppler maps of the lunar surface. How may we obtain information about the third dimension, that is, about the surface-height variations with respect to, say, the mean sphere? We discuss three methods in order of increasing sophistication and usefulness.

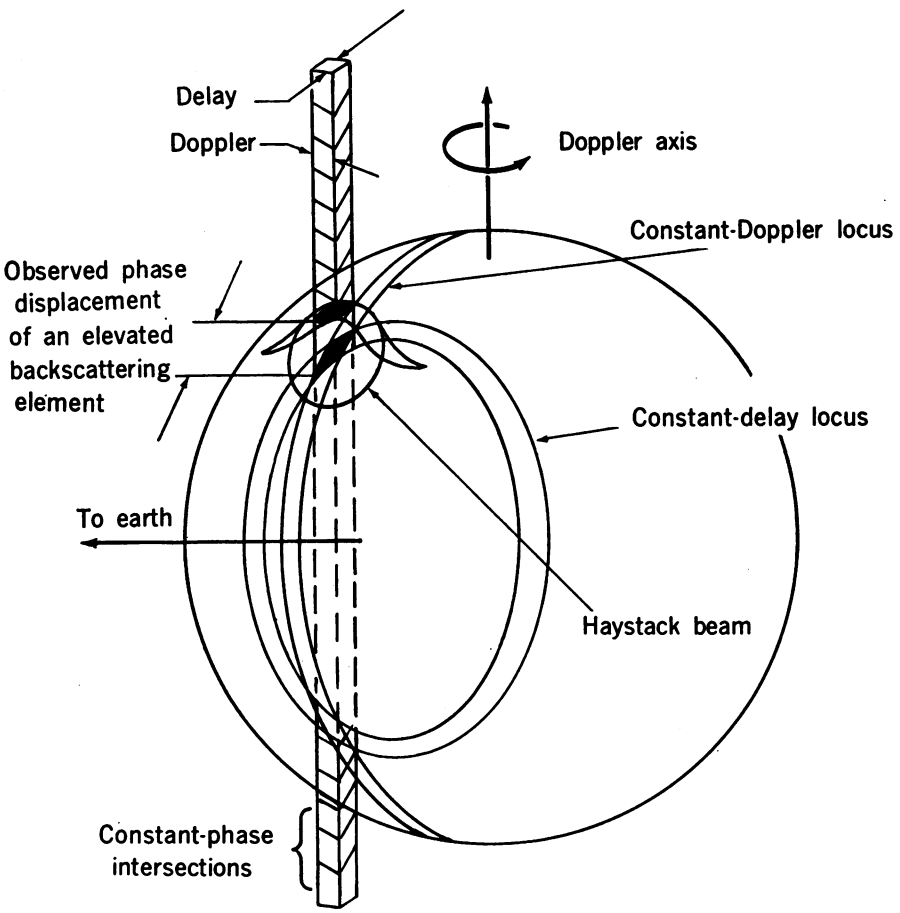

Fig. 1. Coordinate system appropriate for radar determinations of surface heights on the moon. The intersections of planar delay and Doppler contours with the lunar surface would be circles, as shown, were the moon spherical. The hemispheric ambiguity in the intersection of the contours with each other is resolvable by the antenna beam width, except close to the Doppler equator (*6*) where the contour intersections are tangent. Deviations from sphericity are distinguishable interferometrically, as shown, by the displacements of the fringe phase contours from positions that would correspond to the spherical surface initially assumed.

Topography along the Doppler Equator

From the data available in a delay-Doppler map, topographic information can be extracted for the region along the Doppler equator—the plane normal to the Doppler axis (*6*). The basic idea (*12*) can be outlined as follows: For each Doppler resolution slab, the curve of echo power as a function of delay will exhibit a steep rise from the noise level at the delay corresponding to the region near the Doppler equator, followed by a moderately slow decline in echo power for greater delays (*13*). In the noise-free, spherical-target idealization, the first echo received at a given Doppler shift will be from the intersection of the corresponding Doppler slab with the Doppler equator. From a knowledge of the lunar orbit and the moon's rotational motion, one can

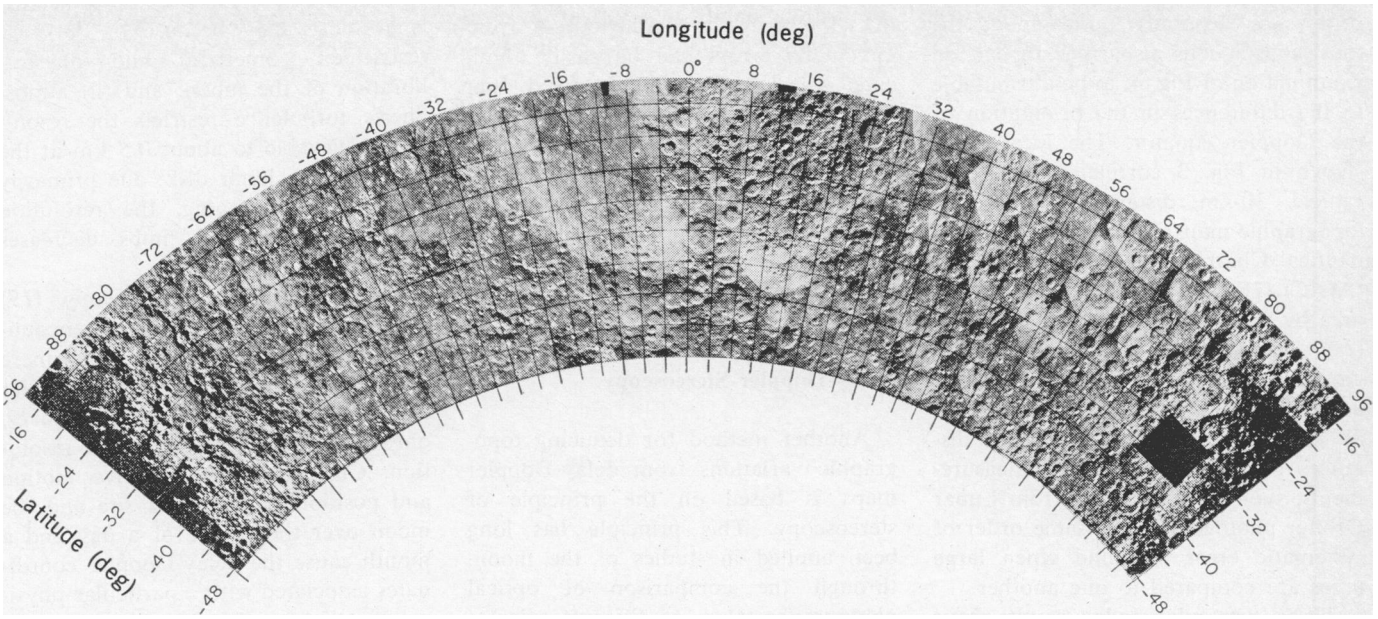

Fig. 2. Radar reflectivity map of a portion of the moon (*10*). Each map element (rectangle) represents a region approximately 2 km on a side on the lunar surface. The coordinates are selenographic latitude and longitude.

predict for each Doppler slab the delay at which the first echo will appear for a given radius of the sphere. (Orbital information is not too critical since one can calibrate all points with respect to the subradar point—the point on the lunar surface pierced by the line from the radar to the moon's center of mass.)

Thus, in the actual case, an estimate of the delay time corresponding to the arrival of the first echo, when compared with the expected arrival time for echoes with that Doppler shift, provides an estimate of the surface-height corresponding to the point of intersection of Doppler slab and Doppler equator. This method has been used at Haystack to develop topographic contours along the Doppler equator of the moon (*14*). The radar signals for these experiments were transmitted in short pulses, each lasting 3 microseconds, with an interpulse period of 30 milliseconds. The echoes were integrated coherently (*4*) for a period of about 10 seconds, yielding a frequency resolution of about 0.1 hertz, or about 2 km when converted to an equivalent distance on the surface of the moon near the subradar point. The postintegration signal-to-noise ratio for the first-arrival echoes is sufficiently great, especially near the subradar point, to allow better accuracy in the height determination than the ± 225 m implied by the 3-μsec pulse length (*15*). A systematic procedure can be developed to exploit this possibility: The echo power as a function of delay for a given Doppler slab can be cross-correlated with an expected profile based on the average radar scattering law for the moon; the delay offset from the expected position for the maximum in the cross-correlation will yield the surface height.

The results obtained with this approach can, in principle, be distorted by (i) the presence of anomalously high topography near, but not on, the Doppler equator; and (ii) the presence near or on the Doppler equator of a surface region with unusual backscattering properties. Such distortive effects can be largely accounted for by carefully comparing the results from a number of observations carried out with different orientations of the Doppler equator and different positions of the subradar point. This redundancy also minimizes the effects of ephemeris errors. Further, "normalization" for each delay-Doppler measurement can be accomplished by assuming that the average shape of the Doppler equator is always spherical and adjusting the set of profiles rigidly in delay to achieve the best match with the reference shape.

Surface-height profiles have already been obtained by this method, but without the use of the cross-correlation procedure described above. Such profiles from sets of observations made almost 2 months apart of the same lunar region are exhibited in Fig. 3; the traces of the Doppler equator on the lunar surface for each date are shown in Fig.

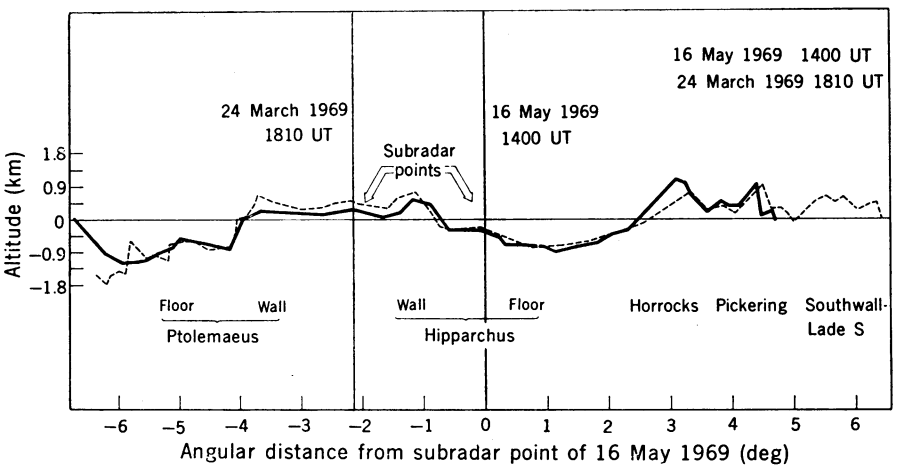

Fig. 3. Lunar topography along the Doppler equator as determined by radar on two separate dates. The major differences between the two surface-height contours are due to actual differences in topography along the neighboring traces of the two Doppler equators (see Fig. 4). *UT*, universal time.

4. The agreement between the two profiles is generally quite good; the most conspicuous disparities appear, on examination of Fig. 4, to be attributable to the differences in the orientation of the Doppler equator. The local relief shown in Fig. 3 correlates well, over typical 30-km distances, with both topographic maps prepared by the Aeronautical Chart and Information Center (ACIC) (*16*) and measurements of this area by the Naval Research Laboratory (*17*). The absolute height and the regional slopes, on the other hand, disagree with the ACIC charts by as much as 2 km over typical correlation distances of 100 km. In other measurements, such as those made from Lunar Orbiter photographs, the same order of systematic error is found when large areas are compared to one another.

These particular radar results have uncertainties of about 3 μsec in the round-trip delay time (corresponding approximately to $\pm$ 225 m in height) since they were not obtained by use of the sophisticated matching technique described above. The more refined analysis could reduce the uncertainties in relative heights to about $\pm$ 100 m or less; the systematic contribution from ephemeris errors can be easily eliminated when a sufficiently improved lunar ephemeris becomes available. With increased radar-system performance, possible through modest improvements in computer capability, the errors in the determination of average heights could be reduced below $\pm$ 50 m, at least near the subradar point.

Delay-Doppler Stereoscopy

Another method for deducing topographic variations from delay-Doppler maps is based on the principle of stereoscopy. This principle has long been applied in studies of the moon, through the comparison of optical photographs taken at different orientations (*18*): By noting the change in the apparent positions of features for different projections, the surface-height contours can be deduced. Applied to optical photographs taken from the earth, the stereoscopy technique has severe limitations: (i) The difference in orientation of the planes of projection is at most $\pm$ 8° because of the very restricted geometrical and physical libration of the moon; and (ii) atmospheric turbulence restricts the resolution achievable to about 0.5 km at the center of the lunar disk; due primarily to the foreshortening, the resolution achievable near the limbs decreases drastically.

In delay-Doppler stereoscopy (*19*) neither of these difficulties is encountered. The limits set by the atmosphere and ionosphere on the delay-Doppler accuracy are reached, for microwaves, only below the meter level of resolution. Changes in the relative motion and position of the radar site and the moon over the course of a day and a month cause the delay-Doppler coordinates associated with a particular physical location to change with time. The delay coordinate, in common with the angle coordinates in the optical case, does not change greatly, due to the limited libration and parallax effects. But the Doppler coordinate changes drastically, as intimated earlier, with the apparent libration axis varying 130° on a typical day and more than 180° on several days each month. Thus, a pair of delay-Doppler measurements, each made with a different orientation of the libration axis, can serve to define the three-dimensional position of a region. The times of observation can be selected to maximize the relative inclination of the delay-Doppler sticks (Fig. 1) that result from the individual measurements, in order to minimize the error in the determination of the coordinates of the intersection point.

But how do we "tag" each region on the moon so that we know to which a given pair of delay-Doppler coordinates applies? Fortunately, as shown in Fig. 2, the moon viewed at radar wavelengths is rich in features as sharply defined as in optical images (Fig. 4). The essential requirement is that these features should appear in the same physical position, independent of the viewing geometry. This condition is vital for the validity of topography determined from a stereoscopic analysis of delay-Doppler data obtained under various kinematic situations. There is no reason to believe that the condition will be seriously violated, at least for regions larger than about 100 m in lateral extent.

Although two separate measurements of delay-Doppler coordinates for each region suffice in principle to determine its three-dimensional position, actual ex-

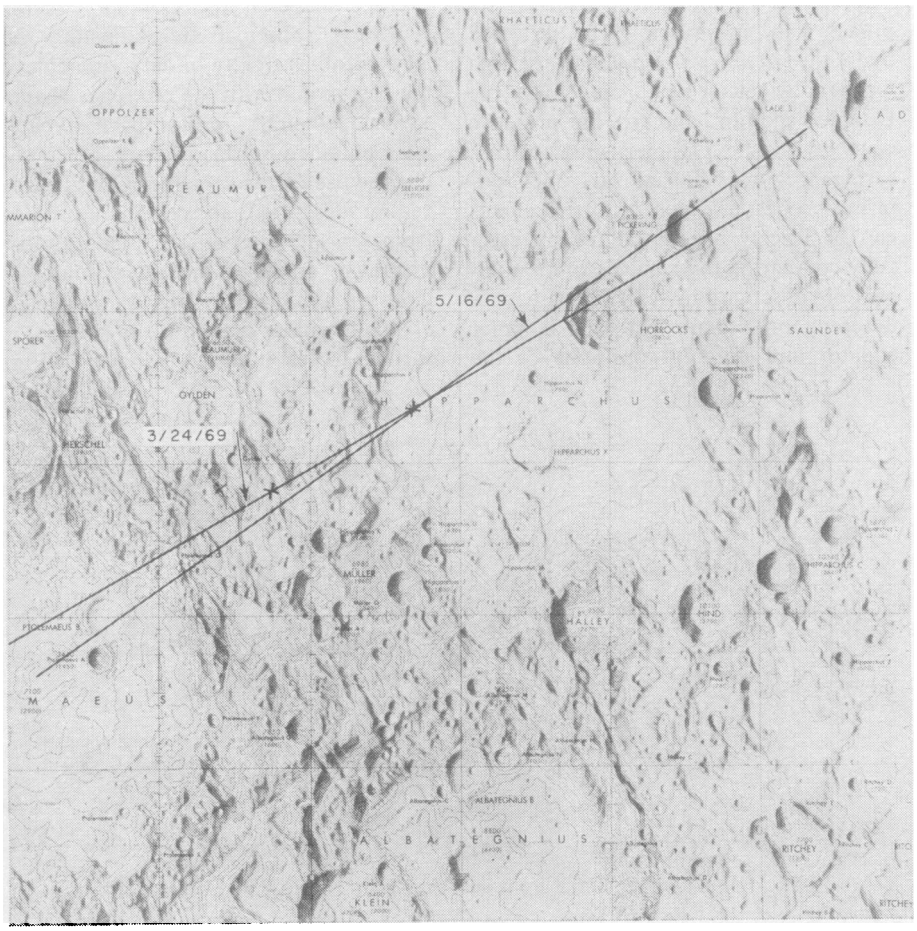

Fig. 4. Traces of the Doppler equators along the lunar surface for the times of observations shown in Fig. 3. The prominent crater Horrocks has selenographic coordinates 4.0°S, 5.9°E.

periments would involve considerable redundancy, both to check consistency and to reduce the effects of random errors of measurement. Not every arbitrarily small region is accessible by this technique because of the lack of distinguishable features at present levels of contrast discrimination. Nonetheless, there is no paucity of such features in any reasonably large part of the visible hemisphere (Fig. 2), and these can form the basis for a global topographic grid.

Since radar features can often be identified unambiguously with optical ones (*20*), the sets of two-coordinate radar measurements can be combined with the complementary optical projections to yield three-dimensional positions. The strong advantage of such a combination is clear: Whereas the undetermined coordinate in the optical photograph lies along the line of sight, the undetermined coordinate in the radar case lies normal to the line of sight. The redundancy afforded by the four coordinates can be used to test the consistency, or reliability, of the topographic deductions.

This method of delay-Doppler stereoscopy has not yet been widely applied; its main use has been to provide calibrations for the three-dimensional radar technique described in the next section. The combined radar-optical method, although possessing considerable promise, has not yet been tried.

Delay-Doppler Interferometry

The most sophisticated and simultaneously most promising technique for determining lunar topography involves the combination of delay-Doppler mapping with radar interferometry (*21*). Aside from the "hemisphere ambiguity" (*4*), which is, in general, eliminated for the moon by the single-antenna resolution, the delay-Doppler coordinates serve to localize the echoing region on a stick, as shown in Fig. 1. The location of this region along the stick can be obtained by interferometry. Thus, suppose two antennas are used interferometrically. If their baseline, when projected onto the plane normal to the earth-moon line, is parallel to the delay-Doppler stick, then maximum resolution will be obtained along the stick. This resolution is given approximately by

$$\delta L = \frac{R\lambda\delta\phi}{2\pi b\cos\theta}$$

where R is the earth-moon distance, $b\cos\theta$ the projection of the baseline (length b) along the plane normal to the earth-moon line, λ the wavelength of the radar signal, and $\delta\phi$ the uncertainty in the determination of the fringe phase (*22*). For λ equal to 3.8 cm and a projected baseline of 1 km, as with the Haystack-Westford radar interferometer, we find that δL is approximately $\pm$ 200 m for an uncertainty of $\pm$ 5° (approximately 0.1 radian) in the fringe phase. Since the radar echo signal is essentially monochromatic, the resolution is ambiguous. The real uncertainty in ϕ is $\delta\phi + 2\pi n$ where n is an unknown integer. But, for the example cited, an ambiguity of 2π corresponds to an ambiguity in distance at the moon of 14 km, which is substantially larger than the initial uncertainty in the third dimension. This illustration demonstrates that a projected baseline of about 1 km, for a radar signal wavelength of about 4 cm, is nearly ideal for the first determinations of the third dimension of the echoing region with interferometry. A much longer baseline would cause ambiguities since the initial uncertainty would then be large compared to the distance equivalent (at the moon) of a 2π change in phase; a much smaller baseline would yield no useful information: The interferometer resolution would be cruder than the prior knowledge of the third dimension. After the uncertainty has been reduced from short-baseline observations, then a longer baseline can be used to improve the resolution. The limits on such a bootstrap procedure are discussed in the next section.

How can the topography actually be determined from these radar observations? To answer this question, we now sketch the procedures used in delay-Doppler interferometry; a mathematical formulation of the theory is given in the Appendix. Two or more antennas can be employed, but for simplicity we shall restrict the discussion to a single pair (*23*). A train of pulses, or a set of phase-coded wave forms of short duration, is transmitted from one antenna toward the moon, with the interval between adjacent pulses adjusted so that the echoes are received interleaved with the transmissions (*24*). The frequency "aliasing" (*4*) introduced by the reciprocal of the interpulse period is rendered harmless by the Doppler shift selection afforded by the antenna beam. The transmissions are circularly polarized with the receiver being set for the opposite sense of circular polarization. Phase coherence is maintained quite rigorously between successive pulses over at least several minutes when the phase of the transmitted wave form is derived from a very stable frequency standard, such as the hydrogen maser used at Haystack. If the two antennas are separated by only a few kilometers the local oscillators in the receivers can also be controlled in a phase-coherent manner by the same frequency standard. For a separation that is too great for direct electrical connections to be feasible, the techniques of long-baseline interferometry (*25*) can, in principle, be employed. However such long baselines have not yet been used in radar interferometry.

The echoes received at each site are sampled, usually at intervals equal to the effective pulse length, and can therefore be sorted separately by relative delay to isolate the first coordinate; from a succession of such echoes from a transmitted train of coherent pulses, segregated by delay, the second (Doppler) coordinate can then be isolated by Fourier analysis. The length of time over which the echoes can be accumulated coherently determines the achievable frequency, or Doppler, resolution and is limited by the frequency stability of the site standard in the otherwise "ideal" situation. (At the present state of the art there are more stringent limits which are discussed in the next section.)

This two-dimensional analysis yields what may be termed a set of complex reflectivities, each member associated with a particular time delay and Doppler shift. Because the two sites are not colocated, a given delay-Doppler coordinate pair would not correspond to the same physical location on the moon or the same orientation of the reflecting element of the surface. To ensure that the correspondence is adequate corrections are made during the processing: We know the difference in delay from any location on the moon to the two sites more than well enough initially to adjust the delay coordinate for the echo signals received, say, at the second site—by altering the sample times—so that the center of the corresponding physical region being observed on the moon will be sampled at the same time in the two sets of received echoes. The Doppler-shift difference can be accommodated accurately enough by rotating the phase of each sample of the echo received at the second site in accord with our prior knowledge of the Doppler difference corresponding to the

site separation and the center of the observed region on the moon. An arbitrary phase error is introduced by this process; however, it does not change from pulse to pulse as the rotations are performed coherently (*26*).

After these corrections are made, the centers of the observed regions will correspond to the same delay-Doppler coordinate pair in the echoes processed at each site. But the other sets of delay-Doppler coordinate pairs will not correspond. To produce the proper correspondence for these, the complex reflectivity for each set of delay-Doppler coordinates from the second site is further rotated in phase by an amount corresponding to the a priori difference appropriate for that particular delay-Doppler cell. If our prior knowledge of the cell location were without error, then corresponding complex reflectivities determined from the echoes received at each site would be identical. In particular, the product of each complex reflectivity by the complex conjugate of its counterpart obtained at the other site would be real. Any residual phase therefore represents the phase error (modulo 2π) in the estimate of the "third coordinate." If this error is known initially to be less than 2π, then the three coordinates—delay, Doppler, and phase—serve in general to define the three spatial coordinates of the physical cell on the moon (*27*). The determination is better the more nearly perpendicular are the directions of constant delay, Doppler, and phase in the region being mapped.

Primarily because of the large excursions of the Doppler equator during each lunation, all areas of the visible hemisphere of the moon approximate the desired conditions reasonably well at some times during the month. Thus, topographic maps of regions of the lunar surface can be produced in a manner analogous to the reflectivity maps described above. Here, of course, the map brightness associated with a resolution cell would be made proportional to its altitude above a reference value rather than to its reflectivity relative to the mean at the corresponding angle of incidence. The latter can be determined from the magnitudes of the products of the corresponding complex reflectivities determined at each site. In Figs. 5 and 6, respectively, maps of height and reflectivity, or backscatter, are shown for the area around the crater Copernicus. In Fig. 5, the brightness (black to white) scale covers heights from 0 to 6 km. A sample comparison of surface-height variations obtained from interferometry with both the results from earth-based optical observations and those from the radar method for the region along the Doppler equator (described above) is given in Fig. 7 (*28*).

We now return to the issue of phase calibration. Earlier we pointed out that, for the region mapped at a given time from coherent processing of the echoes, there is an overall, constant phase uncertainty. It is therefore necessary to have specific cells on the moon to serve as calibration points. At first, one might think that the subradar point could be used to calibrate a set of second-order calibration points distributed over the visible hemisphere. Mainly because of the poor resolution in delay at the subradar point, such an approach is not feasible. One needs a delay-Doppler cell size small compared to the fringe spacing of the interferometer in order to obtain strong fringes, that is, accurate phase data.

Another approach, which is the one being used at the Haystack Observatory, is to select a set of calibration points distributed over the visible surface. These are chosen from among the sharp, well-localized, bright regions that appear on the radar reflectivity maps. The technique of delay-Doppler stereoscopy, discussed above, can be used effectively to determine the three spatial coordinates of these cells, and the interferometry technique can serve to tie together the regions surrounding each calibration point. Similarly, the absolute phase of such regions can be determined by careful calibration of the interferometer, provided there are no 2π

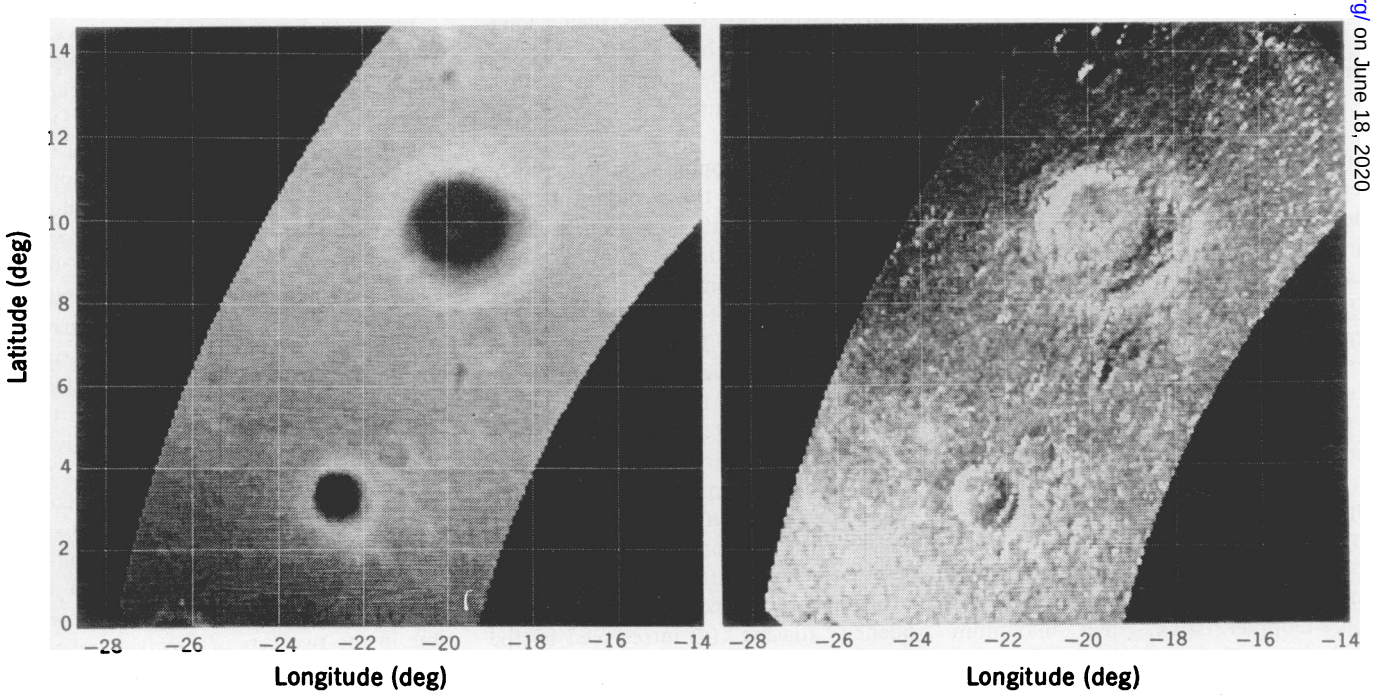

Fig. 5 (left). Map of surface heights determined near the crater Copernicus with the Haystack-Westford radar interferometer. The brightness is proportional to the altitude above the reference height. Full scale (black to white) corresponds to 6 km. The selenographic coordinates of Copernicus are 9.6°N, 20.0°W. The smaller conspicuous crater is Reinhold. Fig. 6 (right). Map of radar reflectivity of the region of the moon shown in Fig. 5. This map was obtained from the same data that yielded the surface heights.

ambiguities introduced by initial uncertainties. The earth's atmosphere, relatively most stable in the winter, is less of a problem here than might be thought because the ray paths to the two elements of a short-baseline interferometer pass through nearly identical parts of the atmosphere. With either method of absolute calibration, overlap areas will, of course, enable consistency to be checked.

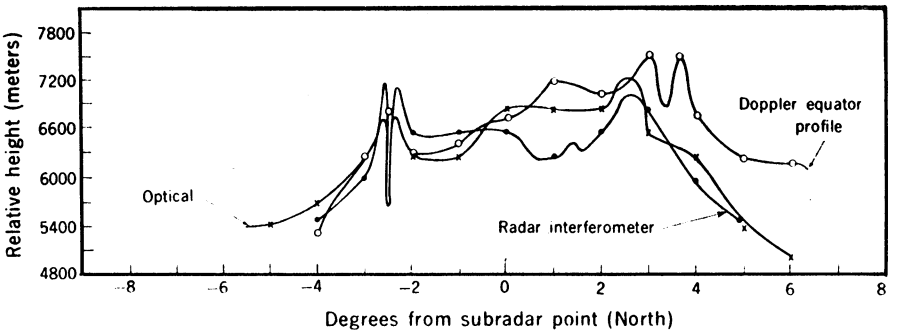

Fig. 7. Comparison of surface heights determined by two radar methods with corresponding results obtained by photogrammetry from earth-based optical observations. The profile extends through the craters Pallas A (6.0°N, 2.2°W) and Ukert A (8.7°N, 1.4°E). The systematically positive slope of the Doppler-equator profile relative to that determined by the interferometer technique is probably due to ephemeris errors, which can be removed when an improved lunar ephemeris becomes available. (Note that the two radar results were obtained from observations several months apart.)

Resolution Limits

We may also inquire about the possible improvements in resolution that might be obtained with this radar technique and the limitations that must be overcome to achieve such resolution in three-dimensional radar photography. The ultimate limit posed by the quantum-mechanical uncertainty principle is too far removed from practicality to be of relevance. The immediate limit is signal-to-noise ratio; beyond this the limit on resolution in the delay component is set at present by the bandwidth limitations of the transmitter, which correspond to a surface resolution of approximately 20 m near the lunar limb. In the Doppler domain, the fundamental limitation is provided by the frequency stability of the oscillators governing signal transmission and echo detection. For an averaging time on the scale of a few seconds to a few hours, a late-model hydrogen maser—the best available frequency standard—has a stability of nearly 1 part in 10^{14}, which implies a maximum frequency resolution of about 10^{-4} hertz at 10 Ghz (X-band) and a corresponding surface resolution of about 5 m in the Doppler component near the subradar point. The minimum integration time required to achieve such a frequency resolution is about 10^{4} seconds! Longer integration times might even be required, depending on the signal strength relative to the system noise temperature and on the phase fluctuations introduced by the changing phase relations of the reflections from the different objects within the physical resolution cell on the target's surface. Depending on how much longer the integration times are, the resolution limit implied by the frequency standard will be that much further from realization. Such severe constraints on integration time imply, of course, that only very limited regions of the lunar surface could be studied at this resolution.

The resolution in the third dimension, given by the fringe phase, depends on the instrumental phase stability and on the separation vector of the interferometer elements. The resolution is also limited by the size—in the fringe-phase "direction"—of the physical lunar region isolated by the delay-Doppler resolution cell. An instrumental phase stability of about 1° is achievable at X-band; for a baseline of 50 km, properly oriented, the corresponding limit on resolution at the lunar surface is about 1 m, if we ignore the slight ambiguity problem. Substantially longer baselines are not practical at X-band because of the consequent loss of correlation between the received echoes from even the smallest resolved elements (*29*).

The phase fluctuations introduced by the earth's atmosphere are far more severe than those due to instrumental instabilities. To decrease drastically such atmospheric effects on "absolute" phase calibration, one can alternate observations of the region under study with those of a suitable first-order calibration point. The switching cycle needs to be short compared to the time scale of the atmospheric fluctuations that would provide the limit on accuracy. The power spectrum of such fluctuations over horizontal paths (*30*), which should provide an upper limit, indicate that cycle times as short as 20 seconds should be quite sufficient. These are within the capabilities of antenna motions; in addition, there would be no difficulty in the maintenance of phase coherence in processing echoes from successive cycles. Since the line of sight from each antenna to any region of the moon would be inclined to the corresponding line for the calibration point by no more than 0.25°, the atmospheric paths will virtually coincide and the phase changes introduced by the atmosphere will cancel almost completely in the comparison with the phase associated with a resolution cell at the calibration point (*31*).

An essential aspect, not previously mentioned, concerns the fact that the delay-Doppler-phase coordinates of a particular physical location on the target change with time. If this change during the interval of coherent integration required to achieve high Doppler resolution is an appreciable fraction of a resolution cell, then it becomes necessary to track each physical element in each of the three coordinates. This necessity always obtains in practice; further, many cells are observed simultaneously—the number depending on the region of the target covered by the antenna beam—and differential tracking of the different cells is required for fine-resolution mapping. Such differential tracking can be accomplished, in principle, in the data processing. At present, however, the uncertainties in the motion of the moon relative to that of the earth would set the limit on achievable resolution because of the "smearing" introduced by these errors into the results of differential tracking. A small resolution cell, as stated, requires a long integration time, and both exacerbate the smearing problem. Two solutions are possible. The relevant parameters of the moon's motion can be estimated from the radar data themselves, or improved values for the orbital and rotational motion can be obtained from laser observations of the lunar retroreflectors and from observations of the ALSEP (Apollo Lunar Surface Experiment Package) transmitters by very-long-baseline interferometry

(VLBI). The accuracy expected from the analysis of the latter data over the next several years should make it unnecessary to implement the first solution and should prevent smearing effects from being the limiting factor in topographic resolution. A side benefit will be the availability of the retroreflectors as independent calibration points.

Another important consideration devolves around the usual necessity to achieve higher time resolution and average signal power than is possible simply by shortening the length of the transmitted pulse. Such resolution is accomplished by phase-coding the transmitted signal and decoding the echo as mentioned earlier. But the resultant fringe-phase determinations are then affected adversely by the echoes from surface elements in the delay "sidelobes." This problem will be especially severe if a bright feature is located in one or more of these sidelobes. However, repeated measurements with, for example, different codes should enable such sidelobe effects to be averaged down to a harmless level.

Other Applications

These techniques of three-dimensional radar photography can also be applied to other celestial bodies. The most attractive possibility is Venus, not only because it is our closest planetary neighbor but also because its surface is visible from the earth only in the radio part of the spectrum. The signal-to-noise requirements are about 10^7 as great for Venus as for the moon, and so the resolution available with earth-based radar will not be as spectacular. Nevertheless, since Venus rotates completely as seen from the earth, the entire planet, and especially the vicinity of the equatorial belt, is accessible for study (*32*). Useful three-dimensional measurements can likely be made near Venus' inferior conjunctions with the new Goldstone radar in California (*33*). Far greater resolution will be obtainable in Puerto Rico with the soon-to-be-improved Arecibo radar telescope and a suitable additional receiver located perhaps 50 to 100 km away (*34*). The effect of fluctuations in Venus' atmosphere on the phase of interferometric signals should not be serious because the paths from any resolution cell on the surface to receivers on the earth could never be separated by more than about 10^{-4} radians and would probably be separated by two orders of magnitude less. Because of these nearly identical paths through Venus' atmosphere, its influence tends to cancel in the comparison of the signals from the different receivers. The effect of the earth's atmosphere, as for observations of the moon, will similarly cancel on comparison of the fringe phase for a particular resolution cell with that for specially chosen calibration points.

Delay-Doppler stereoscopy can also be applied to Venus. For the moon, the main advantage over optical stereoscopy is the far greater range in value of the Doppler coordinate of a particular physical location than of either optical coordinate. For Venus, optical stereoscopy does not suffer from a similar disadvantage (*32*), but it would be inapplicable for earth-based observations because of the poorer resolution in both coordinates that would obtain even if the atmosphere did not completely obscure the surface.

The determinations of global topography from earth-based radar observations are so severely limited by the signal-to-noise ratio that only the inner planets Venus, Mercury, and Mars are conceivable targets for the foreseeable future. Even for them, the polar regions may not be accessible. With the aid of radar systems aboard orbiting spacecraft, however, truly global topographic studies could be made of these bodies, of the hidden hemisphere of the moon, and perhaps of some of the larger satellites of the outer planets as well. The echoes from the signals transmitted by the spacecraft can be detected by suitable combinations of receivers on earth, on the spacecraft, and on other orbiters. The time histories of the positions of the space platforms, needed for proper interpretation of the measurements, can be monitored by phase-stable tracking systems orbiting the earth. For such orbiters, delay-Doppler stereoscopy can also be combined with optical stereoscopy for all of these solar-system objects save for Venus. The main requirement is that the radio and optical images of each surface feature be identifiable with each other unambiouously.

Appendix

We outline here, in mathematical terms, the main principles of delay-Doppler interferometry. Our main object is to determine the location in space of an arbitrary reflecting region on the lunar surface from measurements of the time delay, Doppler shift, and fringe phase of radar echoes from that region. For simplicity, we assume that the orbit and rotation of the moon, the rotation of the earth, the location of the antenna sites, and the instrumental calibrations are all known; further, we neglect the earth's atmosphere. Uncertainties in each of these contributions can be treated separately.

Let $\mathbf{R}_{em}$, $\mathbf{R}_{ei}$ ($i = 1, 2$), and $\mathbf{s}$ represent, respectively, the (time-dependent) vectors from the center of mass of the earth to the center of mass of the moon, from the center of mass of the earth to antenna site i, and from the center of mass of the moon to a point on its surface whose coordinates are to be measured. From these vectors we may form:

$$\mathbf{b} \equiv \mathbf{R}_{e2} - \mathbf{R}_{e1} \tag{1}$$

and

$$\mathbf{R}_i \equiv \mathbf{R}_{em} + \mathbf{s} - \mathbf{R}_{ei}; \qquad i = 1, 2 \tag{2}$$

where $\mathbf{b}$ is the baseline vector, extending from site 1 to site 2, and $\mathbf{R}_i$ is the vector from site i to the observed point on the moon. The time arguments for these vectors are in general all different and in some cases compound. However, we shall suppress these arguments here for convenience; they are readily taken into account in the actual data reduction (*35*). Letting $\mathbf{w}_m$ and $\mathbf{w}_e$ denote the spin angular velocity vectors of the moon and earth, respectively, we have all the quantities we need to determine $\mathbf{s}$ from the time delay, τ, the Doppler shift, f, and the interferometric fringe phase, ϕ, associated with the echoes from the corresponding point on the lunar surface. In terms of these basic vectors, we find (with $\mathbf{r}_1 \equiv \mathbf{R}_1/R_1$)

$$\tau = \frac{2}{c} R_1 \tag{3}$$

$$f = -\frac{2F}{c} \mathbf{V}_1 \cdot \mathbf{r}_1 \tag{4}$$

$$\phi \simeq -\frac{2\pi F}{c} \mathbf{b} \cdot \mathbf{r}_1 \tag{5}$$

when we refer the measurements to site 1 and neglect the motion of the site and the moon during the round-trip time of the radar signals. The quantity F denotes the radar transmitter frequency, c the speed of light, and $\mathbf{V}$ the time derivative of $\mathbf{R}$. In the expression for ϕ, we have retained only the first term in an expansion in powers of (b/R_1); we also ignore any possible ambiguity in ϕ. The expressions for τ and f are well

known; the expression for ϕ represents, in terms of phase, the difference in the times of arrival of a given wave front at the two antennas, referred to the time of arrival at site 1.

Our initial knowledge of **s** is sufficiently good that we need solve only for first-order corrections. With the subscripts o and c denoting, respectively, observed and computed values, the corrections will satisfy:

$$\Delta\tau \equiv \tau_o - \tau_c \simeq \frac{\partial\tau_c}{\partial \mathbf{s}} \cdot \Delta\mathbf{s} \qquad (6)$$

and similar equations for $\Delta f \equiv f_o - f_c$ and $\Delta\phi \equiv \phi_o - \phi_c$, where $\Delta\mathbf{s}$ represents the correction to the initial value assumed for **s**. These partial derivatives can be evaluated approximately by rewriting Eqs. 3 through 5 with the aid of simple vector identities:

$$\tau \simeq \frac{2R}{c}\left\{1 + \frac{\mathbf{r}\cdot\mathbf{s}}{R}\right\} \qquad (7)$$

$$f \simeq -\frac{2F}{c}[\mathbf{V}\cdot\mathbf{r} - (\mathbf{w}_a \times \mathbf{r})\cdot\mathbf{s}] \qquad (8)$$

and

$$\phi \simeq -\frac{2\pi F}{c}[\mathbf{b}\cdot\mathbf{r} - R^{-1}(\mathbf{b}\times\mathbf{r})\times\mathbf{r}\cdot\mathbf{s}] \qquad (9)$$

where

$$\mathbf{R} \equiv \mathbf{R}_{em} - \mathbf{R}_{e1};\ \mathbf{r} \equiv \mathbf{R}/R \qquad (10)$$

$$\mathbf{V} = \mathbf{V}_{em} - \mathbf{w}_e \times \mathbf{R}_{e1} \qquad (11)$$

and

$$\mathbf{w}_a \equiv \mathbf{w}_m + \frac{1}{R}\mathbf{V}\times\mathbf{r} \qquad (12)$$

The first terms on the right sides of Eqs. 7, 8, and 9 represent, respectively, the round-trip time delay from the site to the moon's center, the Doppler shift of echoes from the subradar point, and the fringe phase in the limit $R\to\infty$. Equation 12 gives approximately the apparent angular velocity of the moon as seen from the radar site; the second term is the contribution from the relative orbital motions of site and moon. Returning to the evaluation of the partial derivatives, we express **s** for convenience in time-dependent Cartesian coordinates (x, y, z) referred to an origin at the center of mass of the moon, with axis directions given by unit vectors **(i, j, k)** chosen so that $\mathbf{i} \equiv \mathbf{r}$, $\mathbf{j} \equiv (\mathbf{w}_a \times \mathbf{r})/|\mathbf{w}_a \times \mathbf{r}|$, and $\mathbf{k} = \mathbf{i}\times\mathbf{j}$. The conversion of components to a similar selenocentric coordinate system, at rest with respect to the moon, can be accomplished by means of the appropriate orthogonal transformation after the determination of the first-order corrections to **s** implied by the measurements of τ_o, f_o, and ϕ_o. From Eqs. 6 through 9 it follows after some manipulation that

$$\Delta\mathbf{s}\cdot\mathbf{i} \simeq \frac{c}{2}\Delta\tau \qquad (13)$$

$$\Delta\mathbf{s}\cdot\mathbf{j} \simeq \frac{c}{2F|\mathbf{w}_a\times\mathbf{r}|}\Delta f \qquad (14)$$

and

$$\Delta\mathbf{s}\cdot\mathbf{k} \simeq \frac{c}{2F|\mathbf{w}_a\times\mathbf{r}|}\left(\frac{\mathbf{b}\cdot\mathbf{j}}{\mathbf{b}\cdot\mathbf{k}}\right)\Delta f - \frac{cR}{2\pi F(\mathbf{b}\cdot\mathbf{k})}\Delta\phi \qquad (15)$$

From $s^2 = x^2 + y^2 + z^2$, we deduce the correction Δs to the surface height:

$$\Delta s \simeq \frac{x}{s}\left(\frac{c}{2}\right)\Delta\tau + \frac{c}{2F|\mathbf{w}_a\times\mathbf{r}|}\left[\frac{y}{s} + \frac{z}{s}\left(\frac{\mathbf{b}\cdot\mathbf{j}}{\mathbf{b}\cdot\mathbf{k}}\right)\right]\Delta f - \frac{z}{s}\frac{cR}{2\pi F(\mathbf{b}\cdot\mathbf{k})}\Delta\phi \qquad (16)$$

If the measurements of τ_o, f_o, and ϕ_o are independent and unbiased, with errors of $\sigma(\tau_o)$, $\sigma(f_o)$, and $\sigma(\phi_o)$, respectively, then the standard error in the surface-height correction is, of course, given by the square root of the sums of squares of the three terms on the right side of Eq. 16 with $\sigma(\tau_o)$, $\sigma(f_o)$, and $\sigma(\phi_o)$ replacing $\Delta\tau_o$, Δf_o, and $\Delta\phi_o$, respectively. If redundant data were available, the ensemble would be processed to yield the maximum likelihood estimates of the corrections.

An examination of Eq. 16 shows that the error $\sigma(\Delta s)$ in the height determination will be minimized if $y \simeq 0$ and if $(\mathbf{b}\cdot\mathbf{k}) >> (\mathbf{b}\cdot\mathbf{j})$. The first condition corresponds approximately to the direction of increasing delay being perpendicular to the direction of increasing Doppler shift at the point of interest, as measured on a (spherical) lunar surface. Thus, this point would lie on the same meridian, defined with respect to the Doppler equator, as the subradar point (see Fig. 1). The second condition implies that the baseline vector has a maximum projection in the direction normal to that of increasing Doppler shift, thus affording maximum resolution for this orthogonal component. In summary, maximum accuracy in the determination of Δs is achieved at places where the contours of constant delay, Doppler shift, and fringe phase are mutually orthogonal. Because of the large excursions of the Doppler axis and the motion of the baseline, for the Haystack-Westford system, almost all parts of the visible hemisphere of the moon exhibit this good geometry at some times during a lunation.

A complete discussion of how the radar signals are processed to yield values for $\Delta\tau$, Δf, and $\Delta\phi$ is not possible in the confines of this article, and we restrict discussion simply to the primary concepts not already treated in the literature. Thus, the method for determination of $\Delta\tau$ and Δf—the delay-Doppler corrections—from the echoes received at either site will be omitted (*4*). To determine $\Delta\phi$, the phase of the voltage signal $V_2(t)$ received at site 2 is first transformed to the value $V_2'(t)$ which it would have had if it were received at the reference site and reflected from the center of the observed region:

$$V_2'(t) = V_2(t)\exp[i\Delta\omega_c(t)t] \qquad (17)$$

where

$$\Delta\omega_c(t) \simeq \frac{2\pi F}{c}\frac{d}{dt}(\mathbf{b}\cdot\mathbf{r}_1) \qquad (18)$$

is the a priori value calculated for the difference between the angular frequencies of the signals received at site 1 and site 2. For the Haystack-Westford interferometer, $\Delta\omega_c$ can be as large as 4π sec^{-1}. We ignore here the difference in time of arrival of the wave front at the two sites and the arbitrary phase offset. The former is taken into account by an adjustment in sampling times; the latter will remain constant during the period over which the echoes are integrated coherently and causes no difficulty (see text). The modified signal $V_2'(t)$ is then processed in the standard manner for delay-Doppler mapping (*4*) to produce the (complex) reflectivity $S_2'(\tau, f)$ as a function of the delay and Doppler coordinates τ and f. For each coordinate pair the interferometric fringe phase will be different, and we further transform S_2 by using the a priori value $\phi_c(\tau, f)$ of the differential fringe phase corresponding to the different delay-Doppler resolution cells being observed. Thus,

$$S_2''(\tau,f) = S_2'(\tau,f)\exp[i\phi_c(\tau,f)] \qquad (19)$$

If ϕ_c were exact, then the cross-spectral power

$$P(\tau,f) \equiv S_1^*(\tau,f)S_2''(\tau,f) \qquad (20)$$

would be a real number. Its actual phase is $\Delta\phi$. Its magnitude is the geometric mean of the backscattered power received at sites 1 and 2 from the echoes reflected by the surface element with associated coordinates τ, f.

References and Notes

1. See, for example, V. S. Kislyuk, *Sov. Astron. AJ* **14**, 487 (1970), and references cited therein.
2. Since this work was completed, surface heights on the moon have been obtained by laser altimetry along the great circle in the orbital plane of the Apollo 15 command and service modules. Unpublished, preliminary reports (W. M. Kaula and W. L. Sjogren, personal communication) indicate that these data will yield somewhat higher accuracy than the present results from Earth-based radar.
3. A more complete presentation of results and their geophysical interpretation is given by S. H. Zisk, *Science* **178**, 977 (1972).
4. J. V. Evans and T. Hagfors, Eds., *Radar Astronomy* (McGraw-Hill, New York, 1968).
5. More precisely, the round-trip echo delay serves to locate the echoing region within an ellipsoidal shell whose thickness is half the distance equivalent of the uncertainty in delay. The shell has focuses at the position of the ground antenna at the times of signal transmission and echo reception, and has a major axis equal to the delay. In the present application, relative delays to different portions of the moon are of most relevance; hence relativistic effects, very small to begin with [I. I. Shapiro, *Phys. Rev. Lett.* **13**, 784 (1964)], are completely negligible when only differences are of concern.
6. Here, "apparent velocity" and "apparent angular velocity" denote the values as viewed from a coordinate system fixed to the radar site; they contain contributions both from the relative orbital motion of the radar site and the moon, and from the moon's spin in inerital space. The projection of the apparent angular velocity vector onto the plane normal to the earth-moon vector is called the Doppler axis. The plane that passes through the moon's center of mass and is normal to this axis is the Doppler equatorial plane or Doppler equator. See the Appendix for mathematical details.
7. The actual contours of constant Doppler shift differ from this set of parallel slabs primarily because of parallax: The finite separation of radar and moon causes different surface elements to be at different directions from the radar and produces hyperboloidal Doppler contours. Other effects, such as those of second order in velocity, appear to be negligible for all presently foreseeable mapping purposes.
8. A. E. E. Rogers and R. P. Ingalls, *Science* **165**, 797 (1969).
9. Note that the reflectivity, or backscattered power, for each delay-Doppler cell is expected to fluctuate because of changes in the random phase relations of the echoes from the individual surface scatterers within each cell. These fluctuations are independent of receiver noise and are reduced by averaging over independent observations. Radar maps, more detailed descriptions of the techniques, and a compendium of results can be found in the "Radar Atlas of the Moon" (Report, NASA contract NAS9-7830, M.I.T. Lincoln Laboratory, Lexington, September 1970).
10. This mosaic was obtained from the results contained in the "Radar Atlas of the Moon" (*9*).
11. S. H. Zisk, M. H. Carr, H. Masursky, R. W. Shorthill, T. W. Thompson, *Science* **173**, 808 (1971).
12. This approach was first conceived by A. E. E. Rogers and applied by R. P. Ingalls to the analysis of radar echoes from Venus and Mercury [R. P. Ingalls and L. P. Rainville, *Astron. J.*, in press].
13. For typical curves of echo power as a function of delay for radar echoes from the moon at various radio frequencies, see (*4*).
14. This work was carried out by M. A. Slade and S. H. Zisk.
15. Note that 3 μsec in two-way delay corresponds to 450 m in one-way distance, that is, to $\pm$ 225 m. For a discussion of the dependence of the precision in delay determination on pulse length and signal-to-noise ratio, see G. H. Pettengill, in *Radar Handbook*, M. Skolnick, Ed. (McGraw-Hill, New York, 1970), p. 33-1.
16. The ACIC map [*Lunar Aeronautical Chart 77* (Air Force Aeronautical Chart and Information Center, St. Louis, ed. 1, 1963); *Lunar Aeronautical Chart 59* (Air Force Aeronautical Chart and Information Center, St. Louis, ed. 2, 1966)] was based on optical photogrammetry and shadow measurements.
17. The surface heights measured by the Naval Research Laboratory [A. Shapiro, E. A. Uliana, B. S. Yaplee, S. H. Knowles, in *Moon and Planets*, A. Dollfus, Ed. (North-Holland, Amsterdam, 1968), vol. 2, p. 34] were based on the echo delays from the subradar point.
18. See, for example, Z. Kopal, *The Measure of the Moon* (Gordon & Breach, New York, 1967).
19. This radar application of the stereoscopic technique was suggested for the determination of lunar topography by I. I. Shapiro and, independently, by T. W. Thompson and S. H. Zisk.
20. T. W. Thompson, H. Masursky, R. W. Shorthill, S. H. Zisk, G. L. Tyler, "Contribution No. 16" (Lunar Science Institute, Houston, 1970).
21. This approach for topography determination was suggested by I. I. Shapiro and developed by S. H. Zisk and A. E. E. Rogers; T. W. Thompson pointed out the efficacy of the Haystack-Westford interferometer for this application.
22. See, for example, R. N. Bracewell, in *Handbuch der Physik*, S. Flügge, Ed. (Springer-Verlag, Berlin, 1962), vol. 54, p. 42.
23. If, say, three receiving antennas are located so as to yield baseline projections with substantial components along each of the two relevant orthogonal directions, then two "coordinates" of each reflecting region will be available from the interferometer phases, yielding an overall redundancy in the determination of spatial position.
24. If the echoes are received by two or more antennas, each sufficiently far removed from the transmitter, then the transmissions can be essentially continuous.
25. See, for example, A. E. E. Rogers, *Radio Sci.* **5**, 1239 (1970).
26. The overall phase error for each coherent integration period is removed by a suitable calibration, as discussed below.
27. Note that the phase represents an average of the contributions from each of the scattering elements within the delay-Doppler cell, weighted by the backscattered reflectivities.
28. Aside from the inferences that can be made about the physical properties of the moon from these radar topographic measurements, there is another possibly important application: the mapping of the contour of the lunar limb as viewed from the earth. Precise knowledge of the limb contour is of vital interest in the interpretation of lunar occultation data, both for the study of the structure and position of the occulted objects and for the refinement of the lunar orbit. The radar interferometry technique can, in principle, be applied to this problem in a straightforward way. The difficulty lies primarily in the weakness of the radar echoes from the limb, and secondarily in the necessity to maintain excellent global control to connect accurately the results from individual measurements. Since the delay coordinate adds no direct information on the limb contour, pulse lengths can be extended to increase the effective signal-to-noise ratio and another approach may be used.

    In particular, with the radar beam directed toward a region of the limb containing the Doppler equator, the echo with the largest Doppler shift will emanate from (or nearly from, depending on the limb topography) the point on the limb at the Doppler equator. The value of the Doppler shift and the position of the Doppler equator yield the coordinates of that point on the limb contour. To distinguish such a point from outcroppings near the Doppler equator that have larger Doppler shifts, the second coordinate might be determinable from the interferometric phase of the echo with the largest Doppler shift rather than from the known direction of the Doppler equator. Nonetheless, one measurement would only yield the coordinates of one point on the limb.

    The large excursion of the Doppler equator —a rotation of about 180° with respect to the moon's surface on each of several days during a month—ensures the possibility, in principle at least, of complete limb coverage. But this rapid rotation is not an unmixed blessing because of the consequent limitation on integration time, and hence on Doppler resolution, for a given orientation of the Doppler equator. If the integration time Δt is chosen so that the resolution ΔL along the limb contour is equal to that normal to it, then

    $$\Delta t \simeq (c/2FWv_{rs})^{\frac{1}{2}} \simeq 10 \text{ seconds}$$

    and

    $$\Delta L \simeq (cWs^2/2Fv_{rs})^{\frac{1}{2}} \simeq 1 \text{ km}$$

    where c is the speed of light, F the (assumed X-band) frequency, W the time rate of change of the orientation of the Doppler equator, s the radius of the moon, and v_{rs} the difference in radial velocity between the subradar point and the point at the limb on the Doppler equator. This resolution could be improved at least severalfold by an increase in the signal-to-noise ratio, assumed marginal in the above expressions for ΔL, or by an increase in the radar frequency (note, however, the square-root dependence). It may therefore be possible to produce useful limb contours from radar observations, although a reliable decision in regard to practicality cannot be reached without more detailed analysis.
29. For example, the echoes from a delay-Doppler resolution cell corresponding to a region 2 m square on the moon would yield no fringes for projected baselines of 2×10^7 wavelengths or greater, corresponding to a limit of about 800 km for X-band radar frequencies. To obtain strong fringes a substantially shorter projected baseline would be required. Thus relatively small delay-Doppler cells appear like point sources to the interferometer; the echoes are consequently highly correlated and no fading or scintillation will be encountered.
30. M. C. Thompson, Jr., personal communication.
31. The atmospheric cancellation described earlier is not applicable in virtue of the much greater interferometer baseline involved here.
32. Unfortunately, Venus' Doppler equator is not nearly as accommodating as the moon's and changes its orientation comparatively little, thus restricting the regions in which good resolution can be obtained.
33. R. M. Goldstein, personal communication.
34. G. H. Pettengill, personal communication.
35. For example, if t_1 denotes the time of arrival of a particular wave front of the lunar echo at site 1, the reference site, then the corresponding arrival time for site 2 will be $t_2 \simeq t_1 - \mathbf{b}\cdot\mathbf{r}/c$. Similarly, the argument of $\mathbf{R}_i$ is compound: The vector combination $\mathbf{R}_{em} + \mathbf{s}$ is evaluated at $t_1 - R_i/c$ and the vector $\mathbf{R}_{ei}$ at t_i ($i = 1, 2$). Because the motions of the sites and the moon are very slow compared to the speed of light, these interrelated equations can be solved easily by iteration. In fact, for most applications at most one iteration is required. One additional note of caution is appropriate: All theoretical calculations of observables, including the contributions of orbital motions, must be carried out consistently in a single coordinate system.

36. The Haystack Observatory is supported by NSF grant GP-25865 and NASA grant NGR22-174-003, contract NAS9-7830.

Lunar Topography: Global Determination by Radar: Delay-Doppler stereoscopy and radar interferometry yield high-resolution three-dimensional views of the moon

Irwin I. Shapiro, Martin A. Slade, Stanley H. Zisk, Alan E. E. Rogers and Thomas W. Thompson

Science **178** (4064), 939-948.
DOI: 10.1126/science.178.4064.939